

J | A | C | S

JOURNAL OF THE AMERICAN CHEMICAL SOCIETY

J. Am. Chem. Soc., 1998, 120(12), 2971-2972, DOI:[10.1021/ja9740935](https://doi.org/10.1021/ja9740935)

Terms & Conditions

Electronic Supporting Information files are available without a subscription to ACS Web Editions. The American Chemical Society holds a copyright ownership interest in any copyrightable Supporting Information. Files available from the ACS website may be downloaded for personal use only. Users are not otherwise permitted to reproduce, republish, redistribute, or sell any Supporting Information from the ACS website, either in whole or in part, in either machine-readable form or any other form without permission from the American Chemical Society. For permission to reproduce, republish and redistribute this material, requesters must process their own requests via the RightsLink permission system. Information about how to use the RightsLink permission system can be found at <http://pubs.acs.org/page/copyright/permissions.html>



ACS Publications

MOST TRUSTED. MOST CITED. MOST READ.

Copyright © 1998 American Chemical Society

S.1. Key data for the characterization of the novel compounds.

S.1.1. ^1H and ^{13}C NMR characterization of the $[\text{Re}(\text{CO})_5\{\text{ReH}(\text{CO})_4\}_{2n}]^-$ anions ($n = 2, 3$).

S.1.1.1. ^1H NMR data:

(THF d_8 , 193 K; 11.7 T; the H atoms are numbered starting from the $\text{Re}(\text{CO})_5$ group)

The main key to the identification of the products is provided by the number and the position of the hydridic resonances. As usual in rhenium hydrido-carbonyl clusters, terminal hydrides give resonances at chemical shift values (δ -5/-7) well separated from the bridging ones (δ -16/-17). The signals of the bridging hydrides geminal to the terminal ones are easily identified due to the fast dynamic process observed at higher temperatures. These resonances are about 1 ppm down field with respect to those of the hydrides bridging the inner Re-Re interactions. The assignment of these last resonances has been obtained straightforwardly through 2D-COSY experiments at 193 and 253 K.

The anion 4: δ -5.61 (H4), -16.12 (H3), -16.99 (H1), -17.19 (H2) ppm

Connettivities from 2D-COSY at 193 K (11.7 T and 7.05 T): -16.12 ---> -17.19 ---> -16.99

Coupling features:

-16.99: doublet ($J = 3.0$ Hz) at all the temperatures;

-17.19: unresolved triplet at low temperatures and doublet ($J = 3.0$ Hz) at $T > 233$ K (decoupled by the exchange of the two geminal hydrides on Re5).

The anion 5: δ -5.61 (H6), -15.99 (H5), -17.06 (H2), -17.08 (H1), -17.25 (H4), -17.29 (H3) ppm.

Connettivities from 2D-COSY at 193 K (11.7 T and 7.05 T): -15.99 ---> -17.25 ---> -17.29 ---> -17.06 ---> -17.08

Connettivities from 2D-COSY at 253 K (11.7 T): -16.90 (H1) ---> -17.00 (H2) ---> -17.15 (H3) ---> -17.20 (H4) (at this temperature the signals of H5 and H6 are collapsed)

Coupling features: all the resonances are broad at 193 K but at 253 K they appear as a doublet (-16.90 ppm, $J = 3$ Hz), two unresolved triplets (-17.00 and -17.15 ppm) and a still broad signal at -17.20 ppm (that becomes a doublet at 283 K).

The $[\text{Re}(\text{CO})_5\{\text{ReH}(\text{CO})_4\}_8]^-$ anion and the higher oligomers: they are always in mixture with **4** and **5**, but their existence is sound on the basis of the integration ratios.

The spectral subtraction of the resonances of **4** and **5** (Figure S1) allows the tentative identification of five resonances in the region of the 'inner' bridging hydrides : -17.09 (1), -17.13 (1), -17.18 (1), -17.24 (2), -17.29 (1) ppm. The two geminal hydrides on the terminal rhenium atom are isochronous with those of **4** and **5**. The increase of the length of the chains is expected to cause an increase of the intensity of the highest field signals, attributable to the hydrides in the inner fragments of the chain (two in Re_7 , four in Re_9 , six in Re_{11}).

A "mean length" of the chains in the reaction mixtures can be estimated by the ratio between the overall integrated intensity of the hydridic signals in the region -16.8/-17.2 ppm and either the integral of the signals around -16 ppm (that is the region of the hydrides geminal to the terminal hydrides) or the one of the signals of the terminal hydrides.

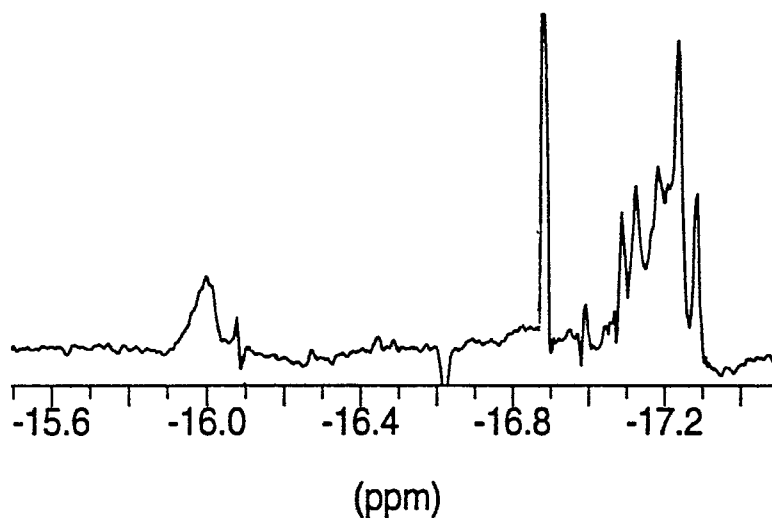
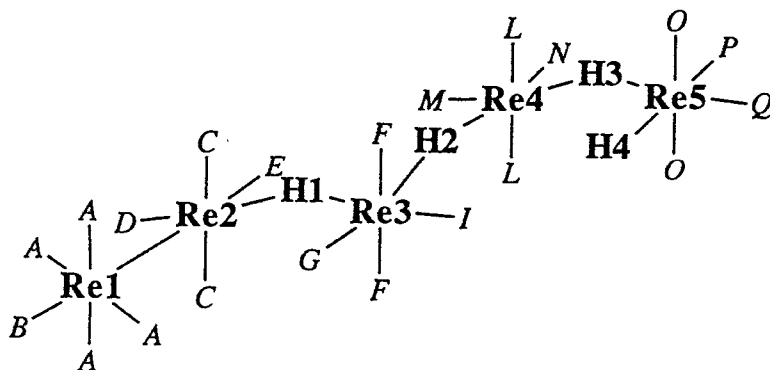


Figure S1. High field hydridic region of the spectrum obtained by spectral subtraction of the signals of compounds **4** and **5** from the spectrum of the mixture obtained with $[\mathbf{1}]/[\mathbf{2}] = 5$ (193 K, 11.7T, $\text{THF-}d_8$). The singlet at -16.9 ppm ca. is due to $[\text{Re}_3(\mu\text{-H})_3(\text{CO})_{12}]$.

S.1.1.2. ^{13}C NMR Characterization of 4.



δ (THF d_8 , 193 K; 4.7 T):	Re1: 197.6 (4), 186.5 (1)
	Re2: 198.62 (2), 193.14 (1), 189.89 (1)
	Re3: 185.09 (2), 182.54 (2)
	Re4: 185.02 (2), 183.76 (1), 183.22 (1)
	Re5: 190.22 (1), 190.08 (2), 188.53 (1).

The above reported attribution of the ^{13}C resonances of 4 have been achieved through the following experiments:

i) the signals of the CO on Re2 and Re3 have been discriminated from those on Re4 and Re5 owing to the preparation of samples selectively enriched in the positions 2,3 or 4,5 (see Figure S2).

ii) The ^1H coupled ^{13}C spectrum allowed the identification of the resonances of the carbonyls *O* and *Q* in the terminal fragment Re5, due to the coupling with the terminal hydride, that is the only hydrogen that gives sizable couplings (with the *cis* carbonyls).

iii) The variable temperature spectra showed an exchange process similar to the one observed for 3, allowing the unambiguous identification of the equatorial carbonyls *P* and *Q* on Re5;

iv) a 2D ^1H - ^{13}C correlation experiment (Figure S3) showed the following cross peaks (^1H with ^{13}C):

-16.12 ppm (H3) with 190.08 (Re5, *O*), 185.02 (Re4, *L*); 183.76 (Re4), 183.22 (Re4) ppm;

-16.99 ppm (H1) with 198.62 (Re2, *C*), 193.14 (Re2), 185.09 (Re3, *F*) and 182.54 ppm (Re3);

-17.19 ppm (H2) with 185.09 (Re3, *F*), 185.02 (Re4, *L*), 183.76 (Re4) and 182.54 ppm (Re3).

v) The low field resonances of intensity 1 (193.14 and 189.89 ppm) observable in the spectrum of the sample selectively enriched at Re2 and Re3 are attributable to the equatorial carbonyls *D* and *E* on Re2, that are indeed the only ones with a singular environment (apart those already identified on

Re5). Moreover, the pattern of the CO resonances on Re2 (and Re1) is quite similar to that observed in the trinuclear chain of **3** (see ref. 4).

vi) The four equivalent carbonyls on Re1 have been identified through their intensity and linewidth (see ref. 4). The peculiar linewidth and temperature behavior allows the assignment also of the signal of relative intensity 1, that on increasing the temperature becomes exceedingly broad and not observable above 240 K.

vii) The measurements of the longitudinal relaxation times at 193 K (4.7 T) indicated that the resonance of relative intensity 2 at 182.54 ppm is likely due to equatorial carbonyls *G* and *I* on Re3 (T_1 312 ms vs T_1 392 ms for the signal at 185.3 ppm, attributed to *F* and *L*) (see ref. 4 and refs. therein).

The specific assignment of the equatorial carbonyls on Re2, Re3 and Re4 could not be achieved.

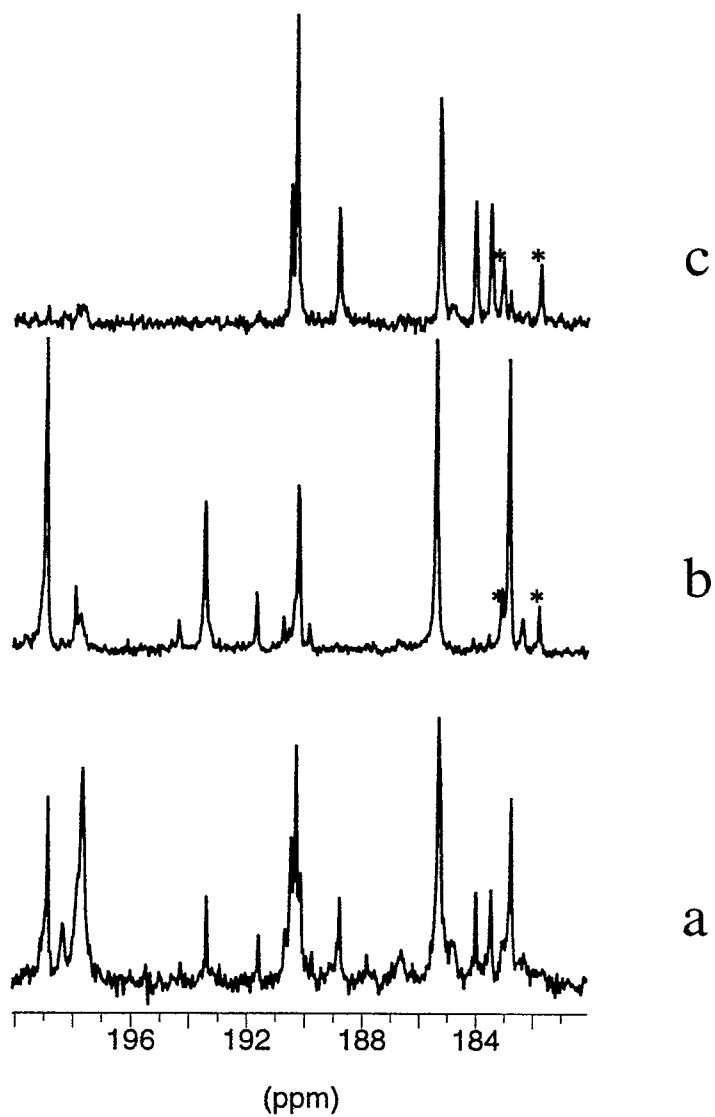


Figure S2. Carbonyl region of the ^{13}C NMR spectra (4.7 T, 193 K, $\text{THF-}d_8$) of compound 4: a) natural abundance; b) selectively enriched at Re2 and Re3; c) selectively enriched at Re4 and Re5. The '*' marks impurities of $[\text{Re}_3(\mu\text{-H})_3(\text{CO})_{12}]$.

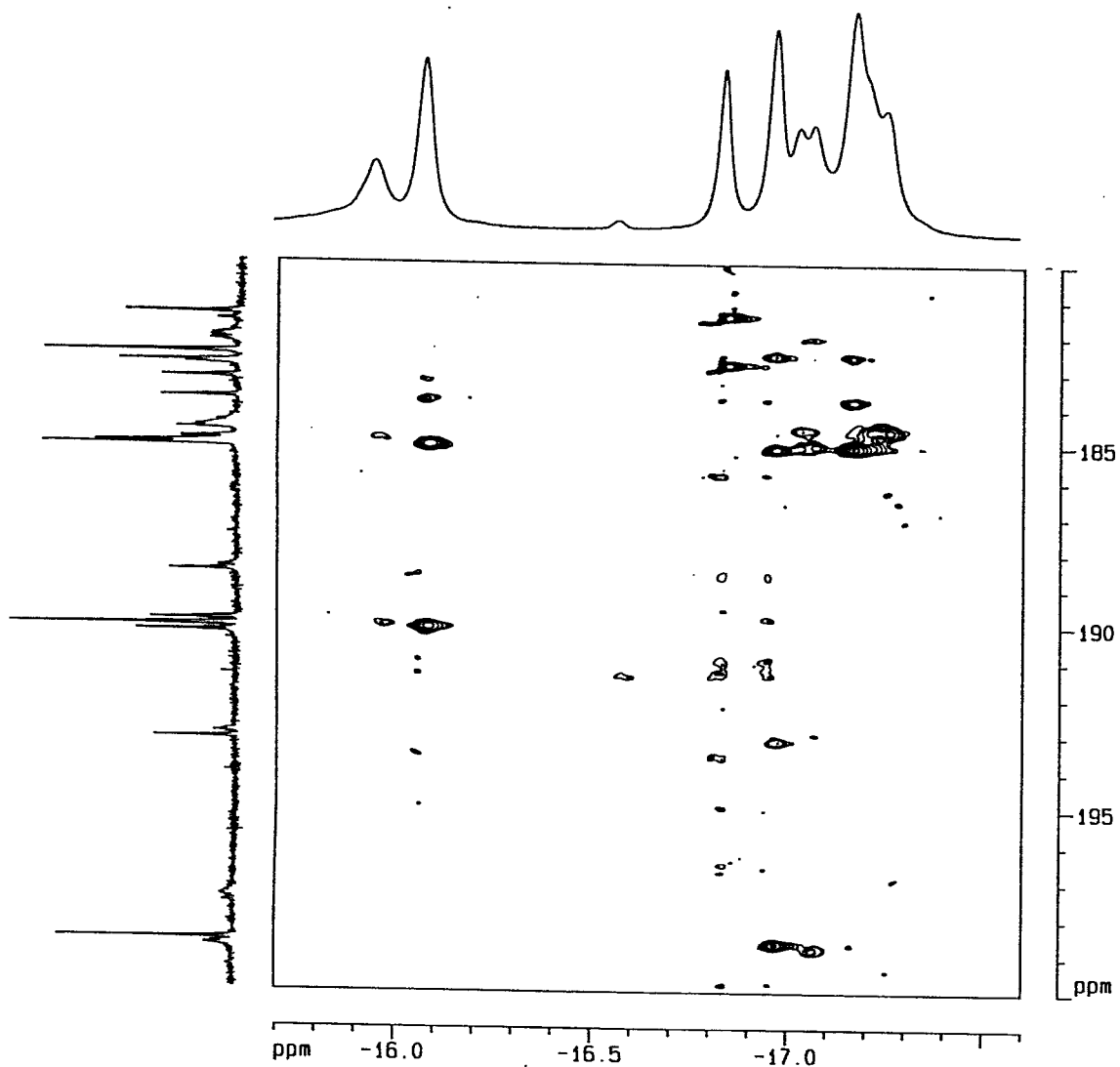
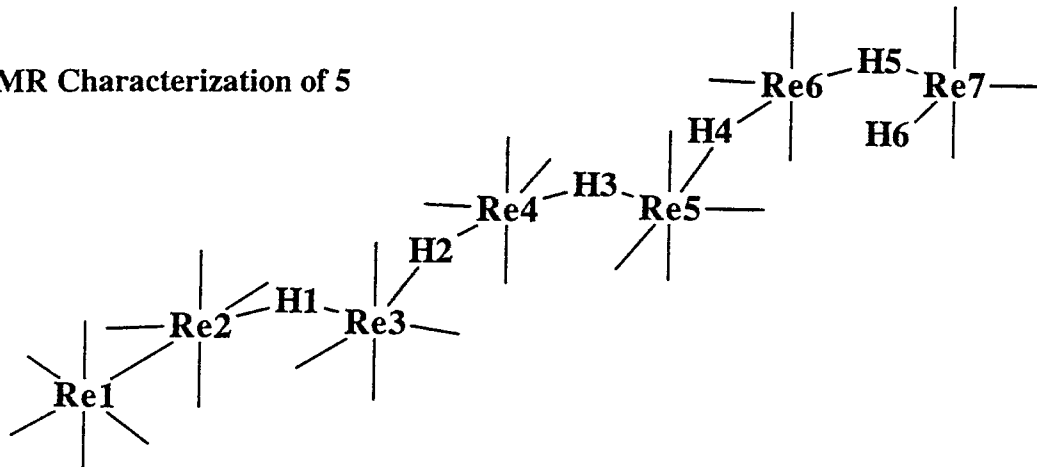


Figure S3. 2D ^1H - ^{13}C inverse correlation of a mixture containing compounds **4** and **5** (ca. 6:4) (7.05 T, 193 K, $\text{THF-}d_8$). 32 transients have been collected over 1K data points for each of the 256 increments in t_1 . The spectral width in F_2 was 840 Hz and in F_1 1660 Hz. The data have been zero filled in F_1 to 1K and weighted with gaussian and shifted sine-bell functions in F_2 and F_1 , respectively.

S1.1.3. ^{13}C NMR Characterization of **5**



The resonances of **5** have been detected by spectral subtractions, since **5** is always in mixture with other oligomers (mostly **4**), see Figure S4.

Analogous spectral subtractions have been used to obtain the spectra of samples selectively ^{13}C O enriched in the (2,3) (Figure S5) or (4,5,6,7) positions (Figure S6).

The 2D ^1H - ^{13}C correlation experiment, at 193 K, (Figure S3 and S7) showed the following cross peaks (^1H with ^{13}C):

H5 (-15.99 ppm) with 190.04 ppm (Re7) and 184.88 ppm (Re6)

H4 (-17.25 ppm) with 184.63 ppm (Re5) and 182.53 ppm (Re5 or Re6)

H3 (-17.29 ppm) with 184.56 ppm

H2 (-17.06 ppm) with 184.56 ppm (Re4), 185.00 ppm (Re3)

H1 (-17.08 ppm) with 198.77 ppm (Re2), 192.96 ppm (Re2), 185.00 ppm (Re3) and 182.04 ppm (Re3)

On these basis the attributions reported below have been established:

Re2 198.77 ppm (2), 192.96 ppm (1), 189.85 ppm (1)

Re3 185.00 ppm (2), 182.11 ppm (1), 182.04 ppm (1)

Re4 + Re5 + Re6 184.88 ppm (2, Re6), 184.63 ppm (2, Re5), 184.56 ppm (2, Re4),

184.4 ppm (1), 182.84 ppm, 182.53 ppm, 182.20 ppm, 181.65 ppm(1)

Re7 190.23 ppm (1), 190.04 ppm (2), 188.39 ppm (1).

For the natural abundance Re1 fragment, only the resonance of the four carbonyls **A** has been detected, at 197.63 ppm.

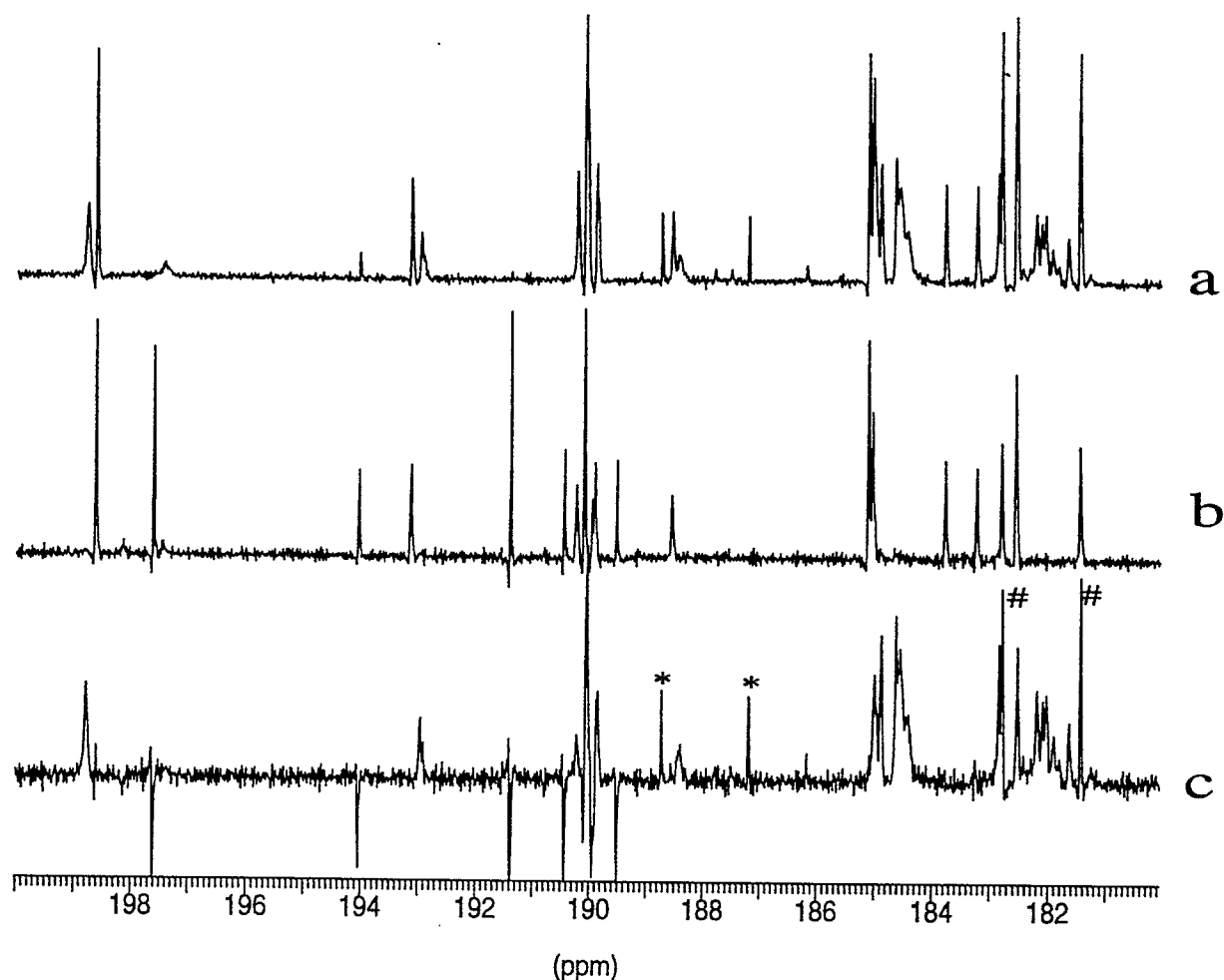


Figure S4. ^{13}C NMR spectra (THF d_8 , 193 K, 7.0 T) (a) of a mixture of ^{13}C O enriched **4** and **5** (ca. 6:4); (b) of a mixture of ^{13}C O enriched **3** and **4** (ca. 5:8) (both obtained from the reaction of natural abundance (PPN)[Re(CO) $_5$] with ^{13}C O enriched **1**); (c) the a - b spectral subtraction, showing in the positive direction the ^{13}C spectrum of **5** and in the negative direction the spectrum of **3**. The signals marked with '*' are due to ^{13}C O enriched [Re $_2(\mu\text{-H})_2(\text{CO})_8$], present in the equilibrium mixture, while those marked with '#' are due to impurities of [Re $_3(\mu\text{-H})_3(\text{CO})_{12}$].

All the spectra have been transformed with resolution enhancement functions (GB=.3 LB=-4).

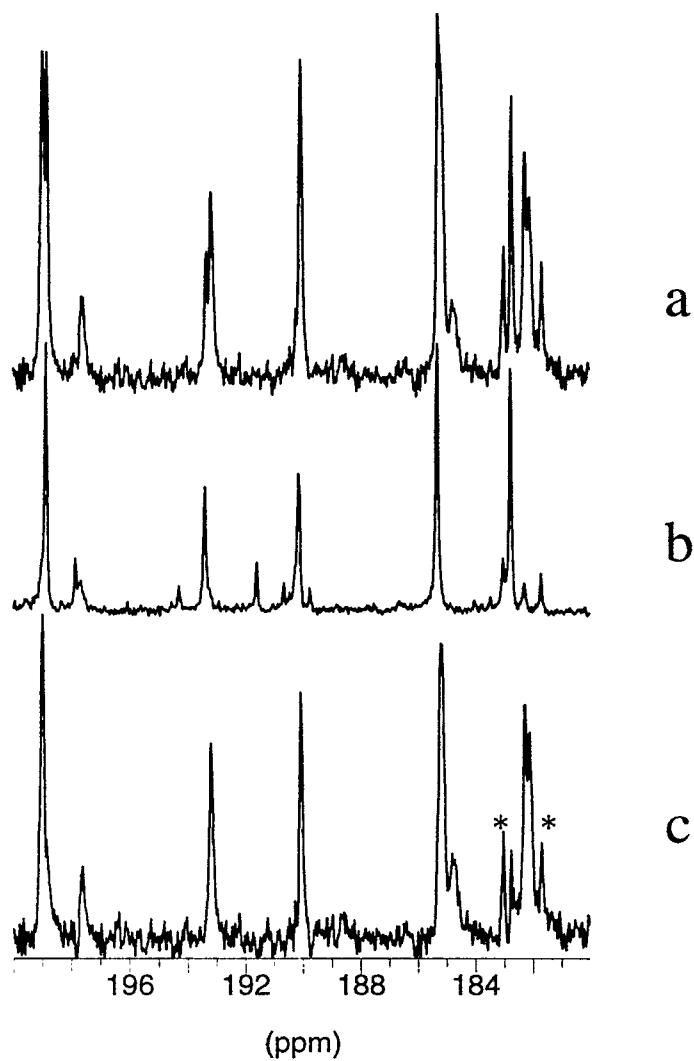


Figure S5. a) Carbonyl region of the ^{13}C NMR spectrum of a mixture of **4** and **5** selectively enriched at Re2 and Re3 (4.7 T, 193 K, $\text{THF-}d_8$). b) The same region in the same condition for a solution of **4**. c) Spectral subtraction a-b, that shows the signals of **5**. A * marks the signals of $[\text{Re}_3\text{H}_3(\text{CO})_{12}]$.

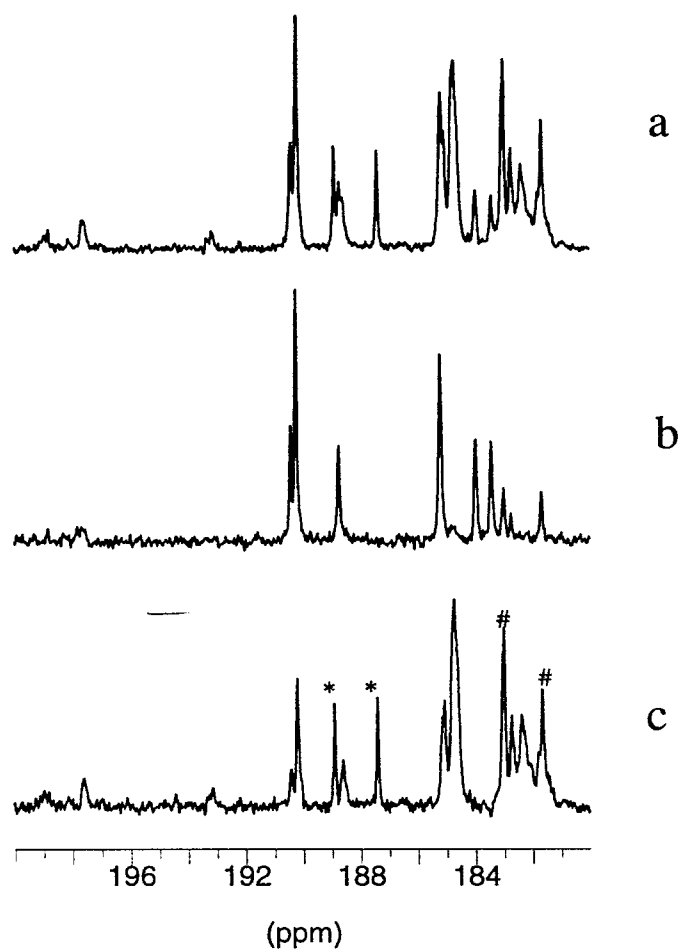


Figure S6. a) Carbonyl region of the ^{13}C spectrum of a mixture of **4** and **5** selectively enriched at positions Re4-Re5 (compound **4**) and Re4-Re5-Re6-Re7 (compound **5**) (4.7T, 193 K, THF-*d*₈). b) The same region in the same conditions for a solution of **4** selectively enriched at positions Re4-Re5. c) Spectral subtraction a-b showing the signal of **5**. The signals marked with '*' are due to enriched $[\text{Re}_2(\mu\text{-H})_2(\text{CO})_8]$, present in the equilibrium mixture, while those marked with '#' are due to impurities of $[\text{Re}_3(\mu\text{-H})_3(\text{CO})_{12}]$.

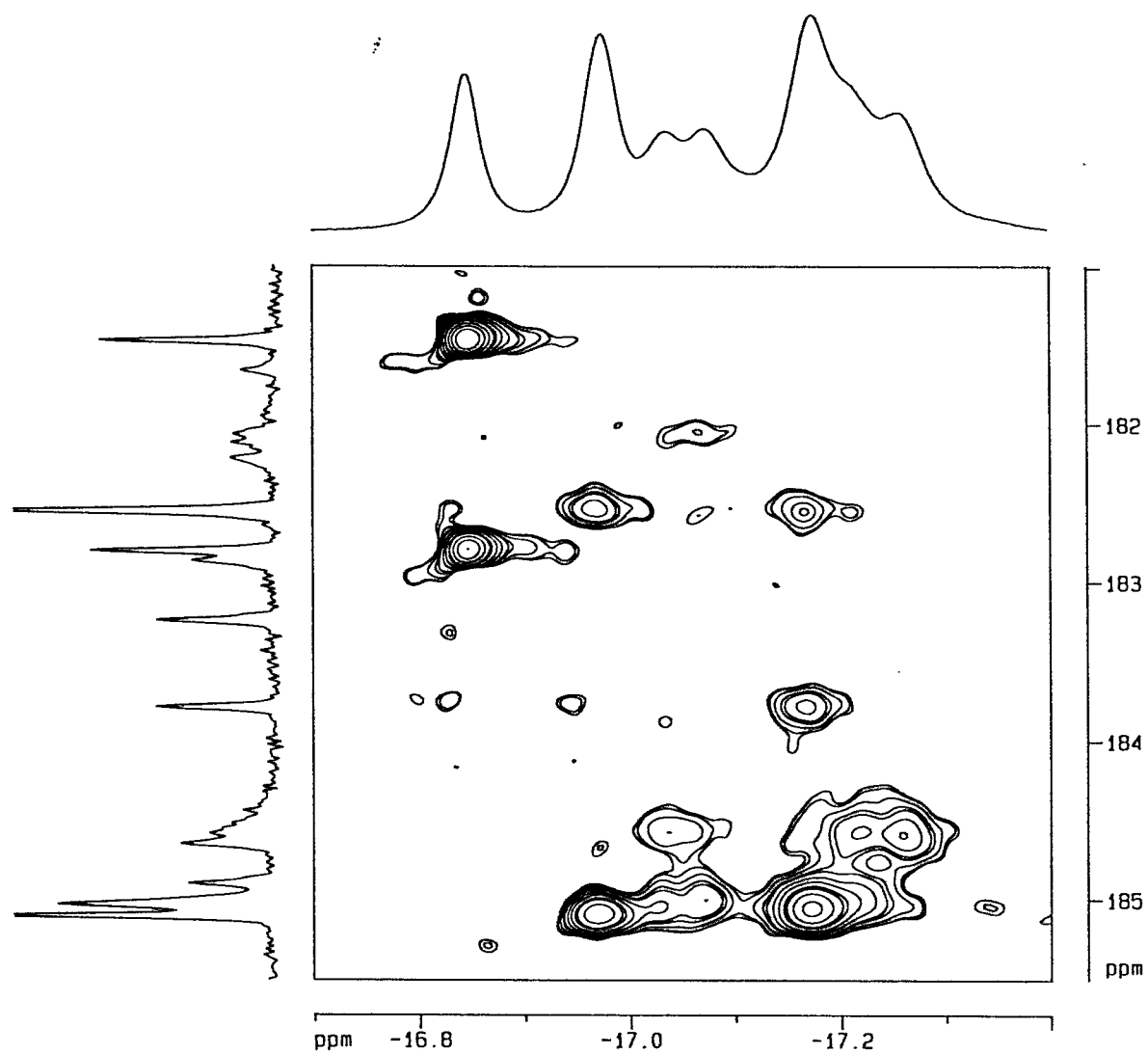


Figure S7. Expanded region of the 2D ^1H - ^{13}C inverse correlation of a mixture containing compounds **4** and **5** (ca. 6:4) (7.05 T, 193 K, $\text{THF-}d_8$) showing the connectivities of the highest field hydrides with the carbonyls in the region 185.5-181.0 ppm.

S1.2 ^1H NMR characterization of the $[\text{Cl}\{\text{ReH}(\text{CO})_4\}_{2n}]^-$ anions.

^1H NMR data for the anions $[\text{Cl}\{\text{ReH}(\text{CO})_4\}_{2n}]^-$ (THF d_8 , 193 K):

$n = 1$, **6**, δ -5.60 (H2), -12.94 (H1) ppm;

$n = 2$, **7**, δ -5.78 (H4), -14.15 (H1), -15.88 (H3), -16.98 (H2) ppm;

$n = 3$, **8**, -5.66 (H6), -14.09 (H1), -15.84 (H5), -16.84 (H2), -17.29 (H3+H4) ppm; at 243 K H3 and H4 give separate resonances (Figure S8).

$n = 4$, **9**, δ -5.63 (H8), -14.09 (H1), -15.90 (H7), -16.84 (H2), -17.29 (H3+H4+H5+H6) ppm.

The attributions of the signals in **6** is straightforward. For the other anions, the attribution of the resonances is facilitated by the low field shift usually underwent by bridging hydrides geminal to chloride ligands (Figure S8). This allows the attribution to H1 of the resonances at δ ca. -14 ppm. A much smaller low field shift is underwent by the resonance of H2 (δ ca. -16.8/-16.9). The signals of the geminal hydrides on the terminal Re atoms are at the usual δ values observed in the previous series of oligomers (δ ca. -6 and -16, for the terminal and bridging hydrides, respectively, in fast exchange at higher temperatures). The remaining $2n-4$ hydrides bridging the inner Re-Re interactions are substantially isochronous. Moreover, all the oligomers of nuclearity higher than 6 give the same five resonances given by **9** [with intensity ratios 1:1:1:1:($2n-4$)], the only difference among the various species being the progressive increase of the integrated intensity of the highest field signal, on increasing the nuclearity. The ratio between this resonance and the overall intensity of the signals at δ -14 (H1) corresponds to $2n-4$, allowing the estimate of a "mean length" of the chain ($2n$, ranging from 4.8 to 7.4 up to ca. 9, as $[\mathbf{1}]/[\text{Cl}^-]$ varies from 3 to 6 to 12).

IR data of the anion **7**:

$\nu(\text{CO})$, THF: 2094w, 2070w, 2023vs, 2011sh, 1999ms, 1970s, 1932m

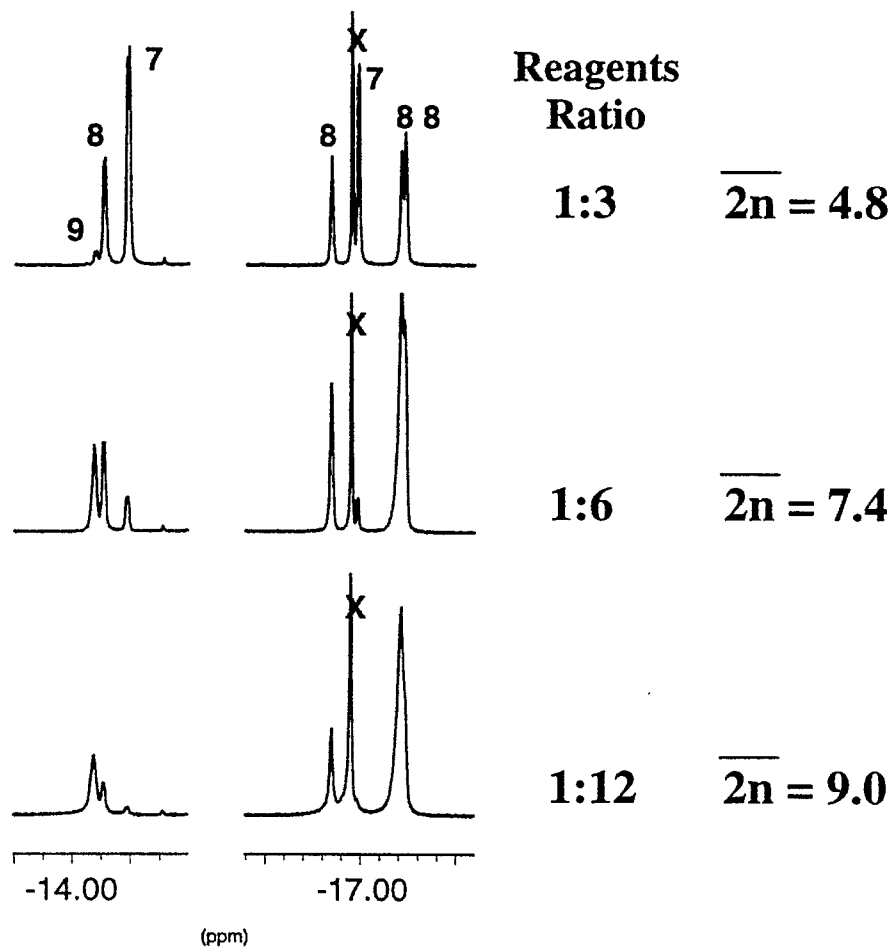


Figure S8 Selected regions of the ^1H NMR spectra (THF d_8 , 243 K) of the mixtures of the $[\text{Cl}\{\text{ReH}(\text{CO})_4\}_{2n}]^-$ anions obtained by treating **1** (0.04 M) with different amounts of (PPN)Cl. The X marks the signal of $[\text{Re}_3(\mu\text{-H})_3(\text{CO})_{12}]$.

Table S2. Summary of crystal data and structure refinement parameters for 7.

formula	$C_{48}H_{48}Cl_2N_2O_{32}Re_8$
formula weight	2725.38
crystal system	Monoclinic
space group	C2/c
a, Å	26.920(3)
b, Å	9.595(1)
c, Å	28.855(3)
β , deg	91.26(1)
V, Å ³	7451.4(14)
Z	4
F(000)	4960
D(calc), g cm ⁻³	2.429
temperature, K	293(2)
diffractometer	SMART
radiation (graph monochr), Å	.71073
absorption coefficient, mm ⁻¹	13.088
crystal size, mm	.78 x .15 x .06
scan method	ω
frame width, deg	.3
max time per frame, s	20
theta range, deg	2.25 to 28.33
index ranges	$-35 \leq h \leq 34, -12 \leq k \leq 12, -37 \leq l \leq 36$
reflections collected	42900
independent reflections	8535 [R(int) = 0.0517]
crystal decay, %	0
absorption correction	SADABS
min. rel transmission	0.482
refinement method	Full-matrix Lst-sqrs on F_o^2
data / restraints / parameters	8535 / 0 / 415
goodness-of-fit on F_o^2	.908
rest goodness-of-fit on F_o^2	.908
R indices [$F_o > 4\sigma(F_o)$]	R1 .0342, wR2 .0661
R indices (all data)	R1 .0565, wR2 .0696
largest diff. peak and hole, e Å ⁻³	1.604 and -1.390
weighting scheme	$w=1/[\sigma^2(F_o^2)+(0.0333P)^2]$

where $P=(F_o^2+2F_c^2)/3$

Table S3. Atomic coordinates and equivalent isotropic displacement parameters [\AA^2] for 7. $U(\text{eq})$ is defined as one third of the trace of the orthogonalized U_{ij} tensor.

	x	y	z	U(eq)
Re(1)	.725174(10)	.51165(3)	.076539(11)	.05292(9)
Re(2)	.603607(9)	.46829(3)	.059609(9)	.04196(8)
Re(3)	.580581(9)	.13578(3)	.085677(9)	.04443(8)
Re(4)	.488299(12)	.16230(3)	.157404(11)	.06393(10)
Cl	.71912(9)	.4277(3)	.15900(8)	.0994(8)
C(11)	.7511(3)	.3251(8)	.0599(3)	.063(2)
C(12)	.7273(3)	.5712(7)	.0142(3)	.065(2)
C(13)	.7927(3)	.5748(9)	.0878(4)	.092(3)
C(14)	.7018(3)	.6986(9)	.0972(3)	.074(2)
C(21)	.6099(2)	.3790(7)	-.0016(3)	.055(2)
C(22)	.5316(3)	.4855(7)	.0545(2)	.051(2)
C(23)	.6108(3)	.6473(7)	.0294(3)	.057(2)
C(24)	.6014(3)	.5540(7)	.1232(3)	.058(2)
C(31)	.5339(2)	.1585(6)	.0320(3)	.051(2)
C(32)	.6343(3)	.0882(7)	.0448(3)	.061(2)
C(33)	.5603(3)	-.0565(7)	.0911(3)	.058(2)
C(34)	.6236(3)	.1137(7)	.1420(3)	.065(2)
C(41)	.4528(3)	.0473(10)	.1108(3)	.082(3)
C(42)	.5202(3)	.0035(9)	.1891(3)	.075(2)
C(43)	.4331(4)	.1623(10)	.1963(4)	.104(3)
C(44)	.5226(4)	.3052(10)	.1956(3)	.108(4)
O(11)	.7682(2)	.2194(6)	.0526(2)	.089(2)
O(12)	.7280(2)	.6085(6)	-.0245(2)	.091(2)
O(13)	.8327(2)	.6119(8)	.0947(3)	.158(4)
O(14)	.6908(2)	.8068(6)	.1094(2)	.102(2)
O(21)	.6134(2)	.3310(6)	-.0381(2)	.081(2)
O(22)	.4899(2)	.4967(6)	.0532(2)	.082(2)
O(23)	.6154(2)	.7507(5)	.0109(2)	.087(2)
O(24)	.5991(2)	.6011(6)	.1591(2)	.083(2)
O(31)	.5055(2)	.1702(6)	.0024(2)	.086(2)
O(32)	.6663(2)	.0623(6)	.0208(2)	.097(2)
O(33)	.5487(2)	-.1704(5)	.0951(2)	.077(2)
O(34)	.6483(2)	.0984(7)	.1744(2)	.109(2)
O(41)	.4324(3)	-.0156(8)	.0831(3)	.129(3)
O(42)	.5379(3)	-.0918(7)	.2082(2)	.108(2)
O(43)	.3970(3)	.1644(9)	.2189(3)	.156(3)
O(44)	.5424(4)	.3900(10)	.2150(3)	.171(4)
N(1)	.8508(3)	.1207(7)	.1913(3)	.084(2)
C(51)	.8242(5)	.024(2)	.2232(5)	.212(8)
C(52)	.7643(5)	.060(2)	.2185(7)	.290(13)
C(53)	.8416(5)	.2794(13)	.1976(6)	.166(6)
C(54)	.8515(6)	.322(2)	.2505(6)	.254(11)
C(55)	.9049(4)	.0960(13)	.2016(5)	.142(5)
C(56)	.9404(5)	.170(2)	.1711(6)	.215(8)
C(57)	.8360(5)	.088(2)	.1416(4)	.141(4)
C(58)	.8451(7)	-.063(2)	.1300(6)	.267(12)
H(1)	.6675	.4076	.0723	.060
H(2)	.6027	.3144	.0978	.060
H(3)	.5315	.2351	.1147	.060
H(4)	.4622	.2925	.1311	.060

H(511)	.8359	.0373	.2549	.254
H(512)	.8301	-.0722	.2145	.254
H(521)	.7461	-.0002	.2384	.347
H(522)	.7531	.0472	.1870	.347
H(523)	.7589	.1555	.2274	.347
H(531)	.8076	.3018	.1886	.199
H(532)	.8635	.3317	.1779	.199
H(541)	.8455	.4204	.2542	.305
H(542)	.8853	.3019	.2592	.305
H(543)	.8296	.2709	.2700	.305
H(551)	.9119	.1236	.2334	.171
H(552)	.9112	-.0033	.1994	.171
H(561)	.9739	.1472	.1806	.258
H(562)	.9355	.2687	.1736	.258
H(563)	.9348	.1414	.1396	.258
H(571)	.8010	.1091	.1367	.169
H(572)	.8548	.1465	.1210	.169
H(581)	.8353	-.0805	.0983	.320
H(582)	.8260	-.1216	.1499	.320
H(583)	.8798	-.0842	.1343	.320

Table S4. Bond lengths [Å] and angles [deg] for 7.

Re(1)-C(12)	1.888(10)
Re(1)-C(13)	1.937(9)
Re(1)-C(11)	1.984(8)
Re(1)-C(14)	1.996(8)
Re(1)-Cl	2.521(2)
Re(1)-Re(2)	3.3243(5)
Re(2)-C(23)	1.938(7)
Re(2)-C(22)	1.949(7)
Re(2)-C(21)	1.974(8)
Re(2)-C(24)	2.014(9)
Re(2)-Re(3)	3.3390(5)
Re(3)-C(33)	1.932(7)
Re(3)-C(32)	1.940(7)
Re(3)-C(31)	1.984(8)
Re(3)-C(34)	1.986(9)
Re(3)-Re(4)	3.2781(5)
Re(4)-C(43)	1.881(9)
Re(4)-C(42)	1.964(10)
Re(4)-C(41)	1.969(10)
Re(4)-C(44)	1.976(10)
C(11)-O(11)	1.135(8)
C(12)-O(12)	1.175(9)
C(13)-O(13)	1.149(9)
C(14)-O(14)	1.138(8)
C(21)-O(21)	1.155(8)
C(22)-O(22)	1.128(7)
C(23)-O(23)	1.134(7)
C(24)-O(24)	1.132(8)
C(31)-O(31)	1.141(8)
C(32)-O(32)	1.147(8)
C(33)-O(33)	1.142(7)
C(34)-O(34)	1.146(9)
C(41)-O(41)	1.136(10)
C(42)-O(42)	1.165(9)
C(43)-O(43)	1.184(9)
C(44)-O(44)	1.116(10)
N(1)-C(55)	1.499(12)
N(1)-C(51)	1.500(13)
N(1)-C(57)	1.513(12)
N(1)-C(53)	1.554(13)
C(51)-C(52)	1.65(2)
C(53)-C(54)	1.60(2)
C(55)-C(56)	1.493(14)
C(57)-C(58)	1.51(2)
C(12)-Re(1)-C(13)	91.0(4)
C(12)-Re(1)-C(11)	91.4(3)
C(13)-Re(1)-C(11)	89.4(3)
C(12)-Re(1)-C(14)	91.6(3)
C(13)-Re(1)-C(14)	88.2(3)
C(11)-Re(1)-C(14)	176.2(3)
C(12)-Re(1)-Cl	177.8(2)
C(13)-Re(1)-Cl	91.2(3)
C(11)-Re(1)-Cl	88.3(2)
C(14)-Re(1)-Cl	88.7(3)

C(12)-Re(1)-Re(2)	87.0(2)
C(13)-Re(1)-Re(2)	168.8(3)
C(11)-Re(1)-Re(2)	101.7(2)
C(14)-Re(1)-Re(2)	80.8(2)
C1-Re(1)-Re(2)	90.85(6)
C(23)-Re(2)-C(22)	90.0(3)
C(23)-Re(2)-C(21)	88.3(3)
C(22)-Re(2)-C(21)	94.3(3)
C(23)-Re(2)-C(24)	93.0(3)
C(22)-Re(2)-C(24)	89.1(3)
C(21)-Re(2)-C(24)	176.3(3)
C(23)-Re(2)-Re(1)	81.2(2)
C(22)-Re(2)-Re(1)	167.2(2)
C(21)-Re(2)-Re(1)	94.7(2)
C(24)-Re(2)-Re(1)	82.2(2)
C(23)-Re(2)-Re(3)	165.7(2)
C(22)-Re(2)-Re(3)	84.8(2)
C(21)-Re(2)-Re(3)	78.9(2)
C(24)-Re(2)-Re(3)	100.1(2)
Re(1)-Re(2)-Re(3)	105.873(10)
C(33)-Re(3)-C(32)	92.3(3)
C(33)-Re(3)-C(31)	89.6(3)
C(32)-Re(3)-C(31)	91.1(3)
C(33)-Re(3)-C(34)	89.6(3)
C(32)-Re(3)-C(34)	92.4(3)
C(31)-Re(3)-C(34)	176.4(3)
C(33)-Re(3)-Re(4)	78.7(2)
C(32)-Re(3)-Re(4)	170.8(2)
C(31)-Re(3)-Re(4)	90.5(2)
C(34)-Re(3)-Re(4)	85.9(2)
C(33)-Re(3)-Re(2)	170.1(2)
C(32)-Re(3)-Re(2)	86.7(2)
C(31)-Re(3)-Re(2)	80.6(2)
C(34)-Re(3)-Re(2)	100.3(2)
Re(4)-Re(3)-Re(2)	102.420(10)
C(43)-Re(4)-C(42)	93.7(4)
C(43)-Re(4)-C(41)	91.7(4)
C(42)-Re(4)-C(41)	94.7(4)
C(43)-Re(4)-C(44)	91.9(4)
C(42)-Re(4)-C(44)	94.9(4)
C(41)-Re(4)-C(44)	169.5(4)
C(43)-Re(4)-Re(3)	174.8(3)
C(42)-Re(4)-Re(3)	84.5(2)
C(41)-Re(4)-Re(3)	83.6(2)
C(44)-Re(4)-Re(3)	93.1(3)
O(11)-C(11)-Re(1)	175.6(7)
O(12)-C(12)-Re(1)	179.2(7)
O(13)-C(13)-Re(1)	179.7(7)
O(14)-C(14)-Re(1)	176.8(7)
O(21)-C(21)-Re(2)	177.8(6)
O(22)-C(22)-Re(2)	177.6(6)
O(23)-C(23)-Re(2)	178.5(7)
O(24)-C(24)-Re(2)	178.4(7)
O(31)-C(31)-Re(3)	177.1(6)
O(32)-C(32)-Re(3)	178.9(6)
O(33)-C(33)-Re(3)	178.7(6)
O(34)-C(34)-Re(3)	178.8(7)
O(41)-C(41)-Re(4)	177.9(10)

O(42)-C(42)-Re(4)	178.4(7)
O(43)-C(43)-Re(4)	176.6(10)
O(44)-C(44)-Re(4)	176.2(10)
C(55)-N(1)-C(51)	104.8(8)
C(55)-N(1)-C(57)	112.9(9)
C(51)-N(1)-C(57)	109.5(9)
C(55)-N(1)-C(53)	106.8(8)
C(51)-N(1)-C(53)	117.1(11)
C(57)-N(1)-C(53)	106.0(9)
N(1)-C(51)-C(52)	107.3(11)
N(1)-C(53)-C(54)	110.0(11)
C(56)-C(55)-N(1)	116.2(10)
C(58)-C(57)-N(1)	111.7(10)

Table S5. Anisotropic displacement parameters [\AA^2] for 7. The anisotropic displacement factor exponent takes the form: $-2 \pi^2 [h^2 a^{*2} U_{11} + \dots + 2 h k a^* b^* U_{12}]$

	U11	U22	U33	U23	U13	U12
Re(1)	.0448(2)	.0510(2)	.0629(2)	-.00847(14)	.00005(13)	.00023(12)
Re(2)	.04370(14)	.04044(14)	.0418(2)	.00261(11)	.00110(11)	.00553(11)
Re(3)	.04683(14)	.03981(14)	.0468(2)	.00029(12)	.00403(12)	.00283(11)
Re(4)	.0729(2)	.0614(2)	.0584(2)	-.0014(2)	.0221(2)	-.0024(2)
C1	.115(2)	.120(2)	.064(2)	.0066(13)	.0078(13)	.027(2)
C(11)	.061(4)	.058(5)	.069(5)	-.003(4)	-.006(4)	.003(4)
C(12)	.061(5)	.042(4)	.092(7)	-.010(4)	.015(5)	.001(3)
C(13)	.058(5)	.089(6)	.130(9)	-.039(6)	.006(5)	-.004(5)
C(14)	.068(5)	.066(5)	.087(7)	-.021(5)	-.003(4)	-.006(4)
C(21)	.056(4)	.048(4)	.062(5)	.011(4)	.008(4)	.010(3)
C(22)	.050(4)	.060(4)	.042(4)	.009(3)	.000(3)	.009(3)
C(23)	.071(5)	.042(4)	.059(5)	.014(3)	.006(4)	.006(3)
C(24)	.055(4)	.056(4)	.063(6)	.011(4)	.000(4)	.006(3)
C(31)	.053(4)	.044(4)	.057(5)	-.005(3)	-.001(4)	-.006(3)
C(32)	.059(4)	.050(4)	.075(6)	-.003(4)	.012(4)	.003(3)
C(33)	.062(4)	.044(4)	.068(5)	-.001(4)	.008(4)	.009(3)
C(34)	.067(5)	.052(4)	.075(6)	.015(4)	-.001(4)	-.006(4)
C(41)	.057(5)	.104(7)	.087(7)	-.021(6)	.013(5)	-.001(5)
C(42)	.084(6)	.071(6)	.071(6)	-.004(5)	.018(5)	-.012(5)
C(43)	.111(7)	.096(7)	.107(8)	.000(6)	.055(7)	.001(6)
C(44)	.171(10)	.093(7)	.062(7)	-.025(5)	.036(7)	-.052(7)
O(11)	.091(4)	.066(4)	.109(5)	-.014(3)	-.014(3)	.025(3)
O(12)	.117(5)	.074(4)	.083(5)	.010(3)	.028(4)	.002(3)
O(13)	.057(4)	.150(7)	.267(11)	-.070(7)	-.018(5)	-.024(4)
O(14)	.112(5)	.064(4)	.131(6)	-.036(4)	.009(4)	.003(3)
O(21)	.097(4)	.092(4)	.053(4)	-.015(3)	.010(3)	.005(3)
O(22)	.045(3)	.117(5)	.083(4)	.016(3)	.007(3)	.024(3)
O(23)	.106(4)	.056(3)	.099(5)	.026(3)	.020(4)	.012(3)
O(24)	.109(4)	.090(4)	.051(4)	-.019(3)	.003(3)	.018(3)
O(31)	.091(4)	.090(4)	.073(4)	-.003(3)	-.033(3)	-.014(3)
O(32)	.087(4)	.077(4)	.130(6)	-.010(4)	.058(4)	.008(3)
O(33)	.095(4)	.043(3)	.094(4)	-.001(3)	.017(3)	.002(3)
O(34)	.106(5)	.124(5)	.094(5)	.039(4)	-.035(4)	-.010(4)
O(41)	.084(5)	.155(7)	.146(7)	-.054(6)	-.004(5)	-.010(4)
O(42)	.136(6)	.096(5)	.092(5)	.027(4)	.008(4)	.009(4)
O(43)	.140(6)	.186(8)	.146(8)	.021(6)	.095(6)	.016(6)
O(44)	.284(12)	.152(7)	.080(6)	-.036(5)	.044(6)	-.111(7)
N(1)	.090(5)	.079(5)	.084(6)	.023(4)	-.021(4)	.002(4)
C(51)	.124(11)	.37(2)	.139(13)	.109(14)	-.026(9)	-.059(13)
C(52)	.104(11)	.41(3)	.35(3)	.18(2)	-.068(14)	-.09(2)
C(53)	.138(11)	.122(11)	.24(2)	.018(11)	-.008(11)	.035(9)
C(54)	.24(2)	.32(2)	.20(2)	-.17(2)	-.06(2)	.05(2)
C(55)	.103(9)	.140(10)	.182(13)	.032(10)	-.027(8)	.020(8)
C(56)	.153(13)	.19(2)	.30(2)	.04(2)	.083(14)	-.053(11)
C(57)	.161(11)	.193(13)	.067(8)	-.001(8)	-.021(7)	-.002(10)
C(58)	.39(3)	.18(2)	.22(2)	-.13(2)	-.12(2)	.05(2)

Table S6. Torsion angles [deg] for 7.

Re(1)-Re(2)-Re(3)-Re(4)	129.376(13)
C(11)-Re(1)-Re(2)-C(21)	-47.3(3)
C(21)-Re(2)-Re(3)-C(31)	-50.5(3)
C(31)-Re(3)-Re(4)-C(41)	40.2(3)
